

Search for CP and P violating pseudoscalar decays into $\pi\pi$

M. Ablikim,¹ M.N. Achasov,⁵ D. Alberto,³⁸ Q. An,³⁶ Z.H. An,¹ J.Z. Bai,¹ R. Baldini,¹⁷ Y. Ban,²³ J. Becker,² N. Berger,¹ M. Bertani,¹⁷ J.M. Bian,¹ O. Bondarenko,¹⁶ I. Boyko,¹⁵ R.A. Briere,³ V. Bytev,¹⁵ X. Cai,¹ A.C. Calcaterra,¹⁷ G.F. Cao,¹ X.X. Cao,¹ J.F. Chang,¹ G. Chelkov,^{15,*} G. Chen,¹ H.S. Chen,¹ J.C. Chen,¹ M.L. Chen,¹ S.J. Chen,²¹ Y. Chen,¹ Y.B. Chen,¹ H.P. Cheng,¹¹ Y.P. Chu,¹ D. Cronin-Hennessy,³⁵ H.L. Dai,¹ J.P. Dai,¹ D. Dedovich,¹⁵ Z.Y. Deng,¹ I. Denysenko,^{15,†} M. Destefanis,³⁸ Y. Ding,¹⁹ L.Y. Dong,¹ M.Y. Dong,¹ S.X. Du,⁴² R.R. Fan,¹ J. Fang,¹ S.S. Fang,¹ C.Q. Feng,³⁶ C.D. Fu,¹ J.L. Fu,²¹ Y. Gao,³² C. Geng,³⁶ K. Goetzen,⁷ W.X. Gong,¹ M. Greco,³⁸ S. Grishin,¹⁵ M.H. Gu,¹ Y.T. Gu,⁹ Y.H. Guan,⁶ A.Q. Guo,²² L.B. Guo,²⁰ Y.P. Guo,²² X.Q. Hao,¹ F.A. Harris,³⁴ K.L. He,¹ M. He,¹ Z.Y. He,²² Y.K. Heng,¹ Z.L. Hou,¹ H.M. Hu,¹ J.F. Hu,⁶ T. Hu,¹ B. Huang,¹ G.M. Huang,¹² J.S. Huang,¹⁰ X.T. Huang,²⁵ Y.P. Huang,¹ T. Hussain,³⁷ C.S. Ji,³⁶ Q. Ji,¹ X.B. Ji,¹ X.L. Ji,¹ L.K. Jia,¹ L.L. Jiang,¹ X.S. Jiang,¹ J.B. Jiao,²⁵ Z. Jiao,¹¹ D.P. Jin,¹ S. Jin,¹ F.F. Jing,³² N. Kalantar-Nayestanaki,¹⁶ M. Kavatsyuk,¹⁶ S. Komamiya,³¹ W. Kuehn,³³ J.S. Lange,³³ J.K.C. Leung,³⁰ Cheng Li,³⁶ Cui Li,³⁶ D.M. Li,⁴² F. Li,¹ G. Li,¹ H.B. Li,¹ J.C. Li,¹ Lei Li,¹ N.B. Li,²⁰ Q.J. Li,¹ W.D. Li,¹ W.G. Li,¹ X.L. Li,²⁵ X.N. Li,¹ X.Q. Li,²² X.R. Li,²⁴ Z.B. Li,²⁸ H. Liang,³⁶ Y.F. Liang,²⁷ Y.T. Liang,³³ G.R. Liao,⁸ X.T. Liao,¹ B.J. Liu,²⁹ B.J. Liu,³⁰ C.L. Liu,³ C.X. Liu,¹ C.Y. Liu,¹ F.H. Liu,²⁶ Fang Liu,¹ Feng Liu,¹² G.C. Liu,¹ H. Liu,¹ H.B. Liu,⁶ H.M. Liu,¹ H.W. Liu,¹ J.P. Liu,⁴⁰ K. Liu,⁶ K. Liu,²³ K.Y. Liu,¹⁹ Q. Liu,³⁴ S.B. Liu,³⁶ X. Liu,¹⁸ X.H. Liu,¹ Y.B. Liu,²² Y.W. Liu,³⁶ Yong Liu,¹ Z.A. Liu,¹ Z.Q. Liu,¹ H. Loehner,¹⁶ G.R. Lu,¹⁰ H.J. Lu,¹¹ J.G. Lu,¹ Q.W. Lu,²⁶ X.R. Lu,⁶ Y.P. Lu,¹ C.L. Luo,²⁰ M.X. Luo,⁴¹ T. Luo,¹ X.L. Luo,¹ C.L. Ma,⁶ F.C. Ma,¹⁹ H.L. Ma,¹ Q.M. Ma,¹ T. Ma,¹ X. Ma,¹ X.Y. Ma,¹ M. Maggiora,³⁸ Q.A. Malik,³⁷ H. Mao,¹ Y.J. Mao,²³ Z.P. Mao,¹ J.G. Messchendorp,¹⁶ J. Min,¹ R.E. Mitchell,¹⁴ X.H. Mo,¹ N. Yu. Muchnoi,⁵ Y. Nefedov,¹⁵ I.B. Nikolaev,⁵ Z. Ning,¹ S.L. Olsen,²⁴ Q. Ouyang,¹ S. Pacetti,¹⁷ M. Pelizaeus,³⁴ K. Peters,⁷ J.L. Ping,²⁰ R.G. Ping,¹ R. Poling,³⁵ C.S.J. Pun,³⁰ M. Qi,²¹ S. Qian,¹ C.F. Qiao,⁶ X.S. Qin,¹ J.F. Qiu,¹ K.H. Rashid,³⁷ G. Rong,¹ X.D. Ruan,⁹ A. Sarantsev,^{15,‡} J. Schulze,² M. Shao,³⁶ C.P. Shen,^{34,§} X.Y. Shen,¹ H.Y. Sheng,¹ M.R. Shepherd,¹⁴ X.Y. Song,¹ S. Sonoda,³¹ S. Spataro,³⁸ B. Spruck,³³ D.H. Sun,¹ G.X. Sun,¹ J.F. Sun,¹⁰ S.S. Sun,¹ X.D. Sun,¹ Y.J. Sun,³⁶ Y.Z. Sun,¹ Z.J. Sun,¹ Z.T. Sun,³⁶ C.J. Tang,²⁷ X. Tang,¹ X.F. Tang,⁸ H.L. Tian,¹ D. Toth,³⁵ G.S. Varner,³⁴ X. Wan,¹ B.Q. Wang,²³ K. Wang,¹ L.L. Wang,⁴ L.S. Wang,¹ M. Wang,²⁵ P. Wang,¹ P.L. Wang,¹ Q. Wang,¹ S.G. Wang,²³ X.L. Wang,³⁶ Y.D. Wang,³⁶ Y.F. Wang,¹ Y.Q. Wang,²⁵ Z. Wang,¹ Z.G. Wang,¹ Z.Y. Wang,¹ D.H. Wei,⁸ Q.G. Wen,³⁶ S.P. Wen,¹ U. Wiedner,² L.H. Wu,¹ N. Wu,¹ W. Wu,¹⁹ Z. Wu,¹ Z.J. Xiao,²⁰ Y.G. Xie,¹ G.F. Xu,¹ G.M. Xu,²³ H. Xu,¹ Y. Xu,²² Z.R. Xu,³⁶ Z.Z. Xu,³⁶ Z. Xue,¹ L. Yan,³⁶ W.B. Yan,³⁶ Y.H. Yan,¹³ H.X. Yang,¹ M. Yang,¹ T. Yang,⁹ Y. Yang,¹² Y.X. Yang,⁸ M. Ye,¹ M.H. Ye,⁴ B.X. Yu,¹ C.X. Yu,²² L. Yu,¹² S.P. Yu Yu,²⁵ C.Z. Yuan,¹ W.L. Yuan,²⁰ Y. Yuan,¹ A.A. Zafar,³⁷ A. Zallo,¹⁷ Y. Zeng,¹³ B.X. Zhang,¹ B.Y. Zhang,¹ C.C. Zhang,¹ D.H. Zhang,¹ H.H. Zhang,²⁸ H.Y. Zhang,¹ J. Zhang,²⁰ J.W. Zhang,¹ J.Y. Zhang,¹ J.Z. Zhang,¹ L. Zhang,²¹ S.H. Zhang,¹ T.R. Zhang,²⁰ X.J. Zhang,¹ X.Y. Zhang,²⁵ Y. Zhang,¹ Y.H. Zhang,¹ Z.P. Zhang,³⁶ Z.Y. Zhang,⁴⁰ G. Zhao,¹ H.S. Zhao,¹ Jiawei Zhao,³⁶ Jingwei Zhao,¹ Lei Zhao,³⁶ Ling Zhao,¹ M.G. Zhao,²² Q. Zhao,¹ S.J. Zhao,⁴² T.C. Zhao,³⁹ X.H. Zhao,²¹ Y.B. Zhao,¹ Z.G. Zhao,³⁶ Z.L. Zhao,⁹ A. Zhemchugov,^{15,*} B. Zheng,¹ J.P. Zheng,¹ Y.H. Zheng,⁶ Z.P. Zheng,¹ B. Zhong,¹ J. Zhong,² L. Zhong,³² L. Zhou,¹ X.K. Zhou,⁶ X.R. Zhou,³⁶ C. Zhu,¹ K. Zhu,¹ K.J. Zhu,¹ S.H. Zhu,¹ X.L. Zhu,³² X.W. Zhu,¹ Y.S. Zhu,¹ Z.A. Zhu,¹ J. Zhuang,¹ B.S. Zou,¹ J.H. Zou,¹ and J.X. Zuo¹

(BESIII Collaboration)

¹*Institute of High Energy Physics, Beijing 100049, China*²*Bochum Ruhr-University, 44780 Bochum, Germany*³*Carnegie Mellon University, Pittsburgh, Pennsylvania 15213, USA*⁴*China Center of Advanced Science and Technology, Beijing 100190, China*⁵*G. I. Budker Institute of Nuclear Physics SB RAS (BINP), Novosibirsk 630090, Russia*⁶*Graduate University of Chinese Academy of Sciences, Beijing 100049, China*⁷*GSI Helmholtzcentre for Heavy Ion Research GmbH, D-64291 Darmstadt, Germany*⁸*Guangxi Normal University, Guilin 541004, China*⁹*Guangxi University, Nanning 530004, China*¹⁰*Henan Normal University, Xinxiang 453007, China*¹¹*Huangshan College, Huangshan 245000, China*¹²*Huazhong Normal University, Wuhan 430079, China*¹³*Hunan University, Changsha 410082, China*

- ¹⁴Indiana University, Bloomington, Indiana 47405, USA
¹⁵Joint Institute for Nuclear Research, 141980 Dubna, Russia
¹⁶KVI/University of Groningen, 9747 AA Groningen, The Netherlands
¹⁷Laboratori Nazionali di Frascati-INFN, 00044 Frascati, Italy
¹⁸Lanzhou University, Lanzhou 730000, China
¹⁹Liaoning University, Shenyang 110036, China
²⁰Nanjing Normal University, Nanjing 210046, China
²¹Nanjing University, Nanjing 210093, China
²²Nankai University, Tianjin 300071, China
²³Peking University, Beijing 100871, China
²⁴Seoul National University, Seoul, 151-747 Korea
²⁵Shandong University, Jinan 250100, China
²⁶Shanxi University, Taiyuan 030006, China
²⁷Sichuan University, Chengdu 610064, China
²⁸Sun Yat-Sen University, Guangzhou 510275, China
²⁹The Chinese University of Hong Kong, Shatin, N.T., Hong Kong
³⁰The University of Hong Kong, Pokfulam, Hong Kong
³¹The University of Tokyo, Tokyo 113-0033 Japan
³²Tsinghua University, Beijing 100084, China
³³Universitaet Giessen, 35392 Giessen, Germany
³⁴University of Hawaii, Honolulu, Hawaii 96822, USA
³⁵University of Minnesota, Minneapolis, Minnesota 55455, USA
³⁶University of Science and Technology of China, Hefei 230026, China
³⁷University of the Punjab, Lahore-54590, Pakistan
³⁸University of Turin and INFN, Turin, Italy
³⁹University of Washington, Seattle, Washington 98195, USA
⁴⁰Wuhan University, Wuhan 430072, China
⁴¹Zhejiang University, Hangzhou 310027, China
⁴²Zhengzhou University, Zhengzhou 450001, China
(Received 25 June 2011; published 11 August 2011)

Using a sample of $(225.2 \pm 2.8) \times 10^6 J/\psi$ events collected with the Beijing Spectrometer at the Beijing Electron-Positron Collider, CP and P violating decays of η , η' , and η_c into $\pi^+\pi^-$ and $\pi^0\pi^0$ are searched for in J/ψ radiative decays. No significant η , η' , or η_c signal is observed, and 90% confidence level upper limits of $\mathcal{B}(\eta \rightarrow \pi^+\pi^-) < 3.9 \times 10^{-4}$, $\mathcal{B}(\eta' \rightarrow \pi^+\pi^-) < 5.5 \times 10^{-5}$, $\mathcal{B}(\eta_c \rightarrow \pi^+\pi^-) < 1.3 \times 10^{-4}$, $\mathcal{B}(\eta \rightarrow \pi^0\pi^0) < 6.9 \times 10^{-4}$, $\mathcal{B}(\eta' \rightarrow \pi^0\pi^0) < 4.5 \times 10^{-4}$, and $\mathcal{B}(\eta_c \rightarrow \pi^0\pi^0) < 4.2 \times 10^{-5}$ are obtained.

DOI: 10.1103/PhysRevD.84.032006

PACS numbers: 11.30.Er, 13.25.Gv, 14.40.Be

I. INTRODUCTION

Finding the source of CP violation is one of the most important goals of particle physics. Violation of CP symmetry has important consequences; it is one of the key ingredients for the matter-antimatter asymmetry in our Universe. CP violation can be experimentally searched for in processes such as meson decays. The decays $\eta/\eta'/\eta_c \rightarrow \pi^+\pi^-$ and $\pi^0\pi^0$, which violate both P and CP invariance, provide an excellent laboratory for testing the validity of symmetries of the physical world. In the standard model, such decays can proceed only via the weak

interaction with a branching fraction of order 10^{-27} , according to Ref. [1]. Higher branching fractions are possible either by introducing a CP violating term in the QCD Lagrangian (a branching fraction up to 10^{-17} can be obtained in this scheme) or allowing CP violation in the extended Higgs sector (in this case, 10^{-15} can be reached), as described in Ref. [1]. The detection of these decays at any level accessible today would signal P and CP violations from new sources, beyond any considered extension of the standard model.

The best previously published results for the η , η' , and η_c decays to $\pi^+\pi^-$ and $\pi^0\pi^0$ are $\mathcal{B}(\eta \rightarrow \pi^+\pi^-) < 1.3 \times 10^{-5}$ [2], $\mathcal{B}(\eta' \rightarrow \pi^+\pi^-) < 2.9 \times 10^{-3}$ [3], $\mathcal{B}(\eta_c \rightarrow \pi^+\pi^-) < 6 \times 10^{-4}$ [4], $\mathcal{B}(\eta \rightarrow \pi^0\pi^0) < 3.5 \times 10^{-4}$ [5], $\mathcal{B}(\eta' \rightarrow \pi^0\pi^0) < 9 \times 10^{-4}$ [6], and $\mathcal{B}(\eta_c \rightarrow \pi^0\pi^0) < 4 \times 10^{-4}$ [4] at the 90% confidence level, respectively.

In this article, results are presented on direct searches for the decays of $\eta/\eta'/\eta_c \rightarrow \pi^+\pi^-$ and $\pi^0\pi^0$ with the

*Also at the Moscow Institute of Physics and Technology, Moscow, Russia.

†On leave from the Bogolyubov Institute for Theoretical Physics, Kiev, Ukraine.

‡Also at the PNPI, Gatchina, Russia.

§Present address: Nagoya University, Nagoya, Japan.

Beijing Spectrometer (BESIII) experiment based on $(225.2 \pm 2.8) \times 10^6 J/\psi$ events [7].

II. BESIII AND BEPCII

BESIII/BEPCII [8] is a major upgrade of the BESII experiment at the Beijing Electron-Positron Collider (BEPC) accelerator [9] for studies of hadron spectroscopy and τ -charm physics [10]. The design peak luminosity of the double-ring e^+e^- collider, BEPCII, is $10^{33} \text{ cm}^{-2} \text{ s}^{-1}$ at a beam current of 0.93 A. The BESIII detector, with a geometrical acceptance of 93% of 4π , consists of the following main components: 1) a small-celled, helium-based main draft chamber with 43 layers. The average single wire resolution is $135 \mu\text{m}$, and the momentum resolution for 1 GeV/ c charged particles in a 1 T magnetic field is 0.5%; 2) an electromagnetic calorimeter (EMC) made of 6240 CsI (TI) crystals arranged in a cylindrical shape (barrel) plus two end caps. For 1.0 GeV photons, the energy resolution is 2.5% in the barrel and 5% in the end caps, and the position resolution is 6 mm in the barrel and 9 mm in the end caps; 3) a time-of-flight system (TOF) for particle identification composed of a barrel part made of two layers with 88 pieces of 5 cm thick, 2.4 m long plastic scintillators in each layer and two end caps with 96 fan-shaped, 5 cm thick, plastic scintillators in each end cap. The time resolution is 80 ps in the barrel and 110 ps in the end caps, corresponding to a K/π separation by more than 2σ for momenta below about 1 GeV/ c ; 4) a muon chamber system made of 1000 m^2 of resistive plate chambers arranged in 9 layers in the barrel and 8 layers in the end caps and incorporated in the return iron yoke of the superconducting magnet. The position resolution is about 2 cm.

The estimation of physics backgrounds is performed with Monte Carlo (MC) simulations. The GEANT4-based simulation software BOOST [11] includes the geometric and material description of the BESIII detectors and the detector response and digitization models, as well as the tracking of the detector running conditions and performance. The production of the J/ψ resonance is simulated by the MC event generator KKMC [12], while the decays are generated by EvtGen [13] for known decay modes with branching fractions being set to the PDG [14] world average values and by Lundcharm [15] for the remaining unknown decays. The analysis is performed in the framework of the BESIII Offline Software System [16] which takes care of the detector calibration, event reconstruction, and data storage.

III. SEARCH FOR η , η' , AND η_c DECAYS INTO $\pi^+\pi^-$

To search for η , η' , and η_c decays into $\pi^+\pi^-$ in J/ψ radiative decays, candidate events with the topology $\gamma\pi^+\pi^-$ are selected using the following criteria. Charged tracks are reconstructed from main draft chamber

hits. To optimize the momentum measurement, we select tracks in the polar angle range $|\cos\theta| < 0.93$ and require that they pass within ± 10 cm of the interaction point in the beam direction and within ± 1 cm of the beam line in the plane perpendicular to the beam. Electromagnetic showers are reconstructed by clustering EMC crystal energies. Efficiency and energy resolution are improved by including energy deposits in nearby TOF counters. Showers identified as photon candidates must satisfy fiducial and shower-quality requirements. The minimum energy is 25 MeV for barrel showers ($|\cos\theta| < 0.8$) and 50 MeV for end cap showers ($0.86 < |\cos\theta| < 0.92$). To exclude showers from charged particles, a photon must be separated by at least 20° from any charged track. EMC cluster timing requirements suppress electronic noise and energy deposits unrelated to the event.

The TOF (both end cap and barrel) and dE/dx measurements for each charged track are used to calculate $\chi_{\text{PID}}^2(i)$ values and the corresponding confidence levels $\text{Prob}_{\text{PID}}(i)$ for the hypotheses that a track is a pion, kaon, or proton, where $i(i = \pi/K/p)$ is the particle type. For pion candidates, we require $\text{Prob}_{\text{PID}}(\pi) > \text{Prob}_{\text{PID}}(K)$ and $\text{Prob}_{\text{PID}}(\pi) > 0.001$.

Candidate events must have two charged tracks with zero net charge, and the number of photons should be greater than or equal to one. The photon candidate with the maximum energy in the e^+e^- center-of-mass frame is taken to be the J/ψ radiative decay photon (γ_{rad}). At least one charged track must be identified as a pion. We do a four-constraint kinematic fit imposing energy and momentum conservation under the $J/\psi \rightarrow \gamma\pi^+\pi^-$ and $J/\psi \rightarrow \gamma K^+K^-$ hypotheses and require $\chi_{\gamma\pi^+\pi^-}^2 < 30$ and $\chi_{\gamma\pi^+\pi^-}^2 < \chi_{\gamma K^+K^-}^2$.

Because of the large branching fraction of $J/\psi \rightarrow \rho\pi$, the decay channel $J/\psi \rightarrow \rho\pi \rightarrow \pi^+\pi^-\pi^0$ constitutes the main source of background. To suppress it and other possible backgrounds with a π^0 , for candidate events with two or more photons, all pairings of the radiative photon and the remaining photons in the event are used to form possible π^0 candidates, and the pairing with its mass closest to the π^0 nominal mass is selected. A clear π^0 signal is observed. To remove it, $m_{\gamma\gamma_{\text{rad}}} < 0.12 \text{ GeV}/c^2$ or $m_{\gamma\gamma_{\text{rad}}} > 0.15 \text{ GeV}/c^2$ is required. The efficiencies of this requirement are 99% for $\eta(\eta') \rightarrow \pi^+\pi^-$ and 96% for $\eta_c \rightarrow \pi^+\pi^-$.

To suppress the $J/\psi \rightarrow e^+e^-$ background and other possible backgrounds with e^+e^- , the requirements of $E_{\pi}^{\text{EMC}} < 1.2 \text{ GeV}$ and $|\chi_{dE/dx}(\pi)| < 3$ are imposed for both π^+ and π^- candidates. Here, E_{π}^{EMC} means the deposited energy of pion candidates in the EMC. $\chi_{dE/dx} = \frac{(dE/dx)_{\text{measured}} - (dE/dx)_{\text{expected}}}{\sigma_{dE/dx}}$, where $(dE/dx)_{\text{measured}}$, $(dE/dx)_{\text{expected}}$, and $\sigma_{dE/dx}$ are the measured, expected, and resolution of the dE/dx values, respectively. To suppress the $J/\psi \rightarrow \mu^+\mu^-$ background, we require

$E_{\pi^+}^{\text{EMC}} > 0.4 \text{ GeV}$ or $E_{\pi^-}^{\text{EMC}} > 0.4 \text{ GeV}$ only in $\eta_c \rightarrow \pi^+ \pi^-$, since its contamination in the low $\pi^+ \pi^-$ mass region is very small. This requirement removes 99.96% of the $J/\psi \rightarrow \mu^+ \mu^-$ background events, while the efficiency is 62.4% for $\eta_c \rightarrow \pi^+ \pi^-$, according to MC simulations.

To avoid possible bias, we first did the background analyses with the signal regions ($m_{\pi\pi} = 0.53\text{--}0.56 \text{ GeV}/c^2$ for $\eta \rightarrow \pi^+ \pi^-$, $0.95\text{--}0.97 \text{ GeV}/c^2$ for $\eta' \rightarrow \pi^+ \pi^-$, and $2.95\text{--}3.02 \text{ GeV}/c^2$ for $\eta_c \rightarrow \pi^+ \pi^-$) blinded to check if all the simulated backgrounds described the data outside of the signal regions. The same was done in the analysis of η , η' , and η_c decay into $\pi^0 \pi^0$ ($m_{\pi\pi} = 0.52\text{--}0.57 \text{ GeV}/c^2$ for $\eta \rightarrow \pi^0 \pi^0$, $0.93\text{--}0.98 \text{ GeV}/c^2$ for $\eta' \rightarrow \pi^0 \pi^0$, and $2.95\text{--}3.02 \text{ GeV}/c^2$ for $\eta_c \rightarrow \pi^0 \pi^0$). Backgrounds from a number of potential background channels listed in the PDG [14] are studied with MC simulations. An inclusive J/ψ MC event sample is also used to investigate other possible surviving background events.

The main nonpeaking backgrounds are from $J/\psi \rightarrow \rho\pi$, $J/\psi \rightarrow \mu^+ \mu^-$, $J/\psi \rightarrow e^+ e^-$, $J/\psi \rightarrow a_2(1320)\pi \rightarrow \gamma\pi^+ \pi^-$, $J/\psi \rightarrow b_1(1235)\pi \rightarrow \gamma\pi^+ \pi^-$, $J/\psi \rightarrow \pi^+ \pi^-$, $J/\psi \rightarrow \gamma\sigma/f_2(1270)/f_0(1500)/f_0(1710) \rightarrow \gamma\pi^+ \pi^-$, and initial state radiation (ISR) events $e^+ e^- \rightarrow \gamma_{\text{ISR}} \pi^+ \pi^-$. The possible peaking backgrounds are $J/\psi \rightarrow \gamma\eta$ with $\eta \rightarrow \gamma\pi^+ \pi^-$ for $\eta \rightarrow \pi^+ \pi^-$, $J/\psi \rightarrow \gamma\eta'$ with $\eta' \rightarrow \gamma\rho^0 \rightarrow \gamma\pi^+ \pi^-$ for $\eta' \rightarrow \pi^+ \pi^-$, and $J/\psi \rightarrow \gamma\eta_c$ with $\eta_c \rightarrow \gamma\pi^+ \pi^-$ for $\eta_c \rightarrow \pi^+ \pi^-$. Branching fractions of $J/\psi \rightarrow \gamma\eta \rightarrow \gamma\gamma\pi^+ \pi^-$ and $J/\psi \rightarrow \gamma\eta' \rightarrow \gamma\gamma\pi^+ \pi^-$ have been measured [14]. After event selection, the contribution from the decay $J/\psi \rightarrow \gamma\eta \rightarrow \gamma\gamma\pi^+ \pi^-$ to the background is less than 11 events within a mass region of $\pm 2\sigma$ around the η mass peak. Since the $\pi^+ \pi^-$ mass distribution is smooth, this background may be neglected. The contamination from the $J/\psi \rightarrow \gamma\eta' \rightarrow \gamma\gamma\pi^+ \pi^-$ background channel will be fixed in the fit below. As for the possible peaking background $\eta_c \rightarrow \gamma\pi^+ \pi^-$ for $\eta_c \rightarrow \pi^+ \pi^-$, this process is Okubo-Zweig-Iizuka suppressed, unlike $\eta/\eta' \rightarrow \gamma\pi^+ \pi^-$, and can only happen by $c\bar{c}$ annihilation, and the photon must be from the final state quark. The branching fraction for such a process is

expected to be very small. It was calculated to be $\mathcal{B}(\eta_c \rightarrow \gamma\pi^+ \pi^-) = 4.5 \times 10^{-6}$ in Ref. [17] in the framework of nonrelativistic QCD. After QED contributions are taken into account, the $\mathcal{B}(\eta_c \rightarrow \gamma\pi^+ \pi^-)$ becomes 1.5×10^{-6} . With these calculated branching fractions, the contribution from this peaking background after event selection can be neglected.

Figure 1 shows the $\pi^+ \pi^-$ invariant mass distributions of the final candidate events in the η , η' , and η_c mass regions after removal of the blinded boxes, where dots with error bars are data, and the dashed histograms are all the simulated normalized backgrounds. No evident signal is observed, and the simulated backgrounds describe the data well. For $\eta \rightarrow \pi^+ \pi^-$, a fit with an η signal shape obtained from MC simulation and a 2nd-order Chebychev function as the background shape gives 17 ± 23 signal events with a statistical significance of 0.8σ . For $\eta' \rightarrow \pi^+ \pi^-$, by fitting the $\pi^+ \pi^-$ invariant mass spectrum with the MC determined shape for the η' signal, the normalized mass distribution from $J/\psi \rightarrow \gamma\eta' \rightarrow \gamma\gamma\pi^+ \pi^-$ as the only peaking background, and a 2nd-order Chebychev function for other backgrounds, 0.1 ± 15 events are obtained with a statistical significance of 0.1σ . For $\eta_c \rightarrow \pi^+ \pi^-$, a fit with an acceptance-corrected η_c signal shape obtained from MC simulation and a 3rd-order Chebychev function as the background shape gives 52 ± 35 signal events with a statistical significance of 1.5σ . The fitted results are shown in Fig. 1 with solid lines, where the arrows show the signal mass regions which contain 95% of the signal according to MC simulations.

We determine a Bayesian 90% confidence level upper limit on N_{sig} by finding the value $N_{\text{sig}}^{\text{UP}}$ such that

$$\frac{\int_0^{N_{\text{sig}}^{\text{UP}}} \mathcal{L} dN_{\text{sig}}}{\int_0^{\infty} \mathcal{L} dN_{\text{sig}}} = 0.90,$$

where N_{sig} is the number of signal events, and \mathcal{L} is the value of the likelihood as a function of N_{sig} . The upper limits on the numbers of η , η' , and η_c are determined to be 48, 32, and 92, respectively.

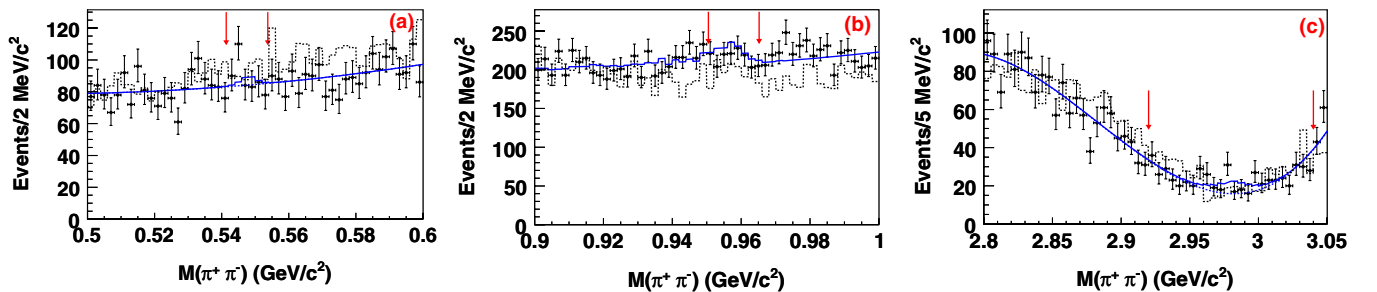


FIG. 1 (color online). (a)–(c): The $\pi^+ \pi^-$ invariant mass distributions of the final candidate events in the η , η' , and η_c mass regions, respectively. The dots with error bars are data, the solid lines are the fit described in the text, and the dashed histograms are the sum of all the simulated normalized backgrounds. The arrows show mass regions which contain around 95% of the signal according to MC simulations.

IV. SEARCH FOR η , η' , AND η_c DECAYS INTO $\pi^0\pi^0$

To search for η , η' , and η_c decays into $\pi^0\pi^0$ in J/ψ radiative decays, candidate events with the topology $\gamma\pi^0\pi^0$ are selected using the following selection criteria. An event must have 5 or 6 photons and no charged tracks. Here, in selecting photons, the EMC cluster timing requirement is not used. For the $\eta/\eta' \rightarrow \pi^0\pi^0$ modes, the photon with the maximum energy is identified as the radiative photon, and all the other remaining photons in the event are used to form two π^0 candidates. For $\eta_c \rightarrow \pi^0\pi^0$, for photons with $E < 0.3$ GeV (a potential radiative photon), all possible two-photon pairings of the remaining photons in the event are used to form two π^0 candidates. If there is more than one radiative photon candidate ($E < 0.3$ GeV), the one that gives the smallest $|m_{5\gamma} - m_{J/\psi}|$ is used. The candidate event is chosen as the photon pairing combination giving the minimum $\chi = \sqrt{(m_{\gamma\gamma_1} - m_{\pi^0})^2 + (m_{\gamma\gamma_2} - m_{\pi^0})^2}$. End cap-end cap combinations are of lower quality and only make up about 0.7% of all the π^0 candidates, so they are removed. The $\gamma\gamma$ invariant masses are required to satisfy $|m_{\gamma\gamma} - m_{\pi^0}| < 0.01625$ GeV/ c^2 ($\sim 2.5\sigma$) for $\eta(\eta') \rightarrow \pi^0\pi^0$ and $|m_{\gamma\gamma} - m_{\pi^0}| < 0.0175$ GeV/ c^2 ($\sim 2.5\sigma$) for $\eta_c \rightarrow \pi^0\pi^0$. To improve the $\pi^0\pi^0$ mass resolution, especially for the $\eta(\eta') \rightarrow \pi^0\pi^0$ mode, a four-constraint kinematic fit under the $J/\psi \rightarrow \gamma\pi^0\pi^0$ hypothesis is done. To suppress backgrounds with a $\omega(\rightarrow \gamma\pi^0)$, events with the invariant mass of $\gamma\pi^0$ satisfying $0.72 < m_{\gamma\pi^0} < 0.82$ GeV/ c^2 are rejected.

The main backgrounds with π^0 signals are from $J/\psi \rightarrow a_2(1320)\pi \rightarrow \gamma\pi^0\pi^0$, $J/\psi \rightarrow b_1(1235)\pi \rightarrow \gamma\pi^0\pi^0$, $J/\psi \rightarrow \omega\pi^0(\pi^0)$ with $\omega \rightarrow \gamma\pi^0$, and $J/\psi \rightarrow \gamma\sigma/f_2(1270)/f_0(1500)/f_0(1710)/f_4(2050) \rightarrow \gamma\pi^0\pi^0$. Non- π^0 background contributions are represented by the normalized number of events in the sidebands of the two π^0 mass distributions, where the two π^0 mass sidebands are defined as $0.084 < m_{\gamma\gamma} < 0.098$ GeV/ c^2 or $0.168 < m_{\gamma\gamma} < 0.182$ GeV/ c^2 .

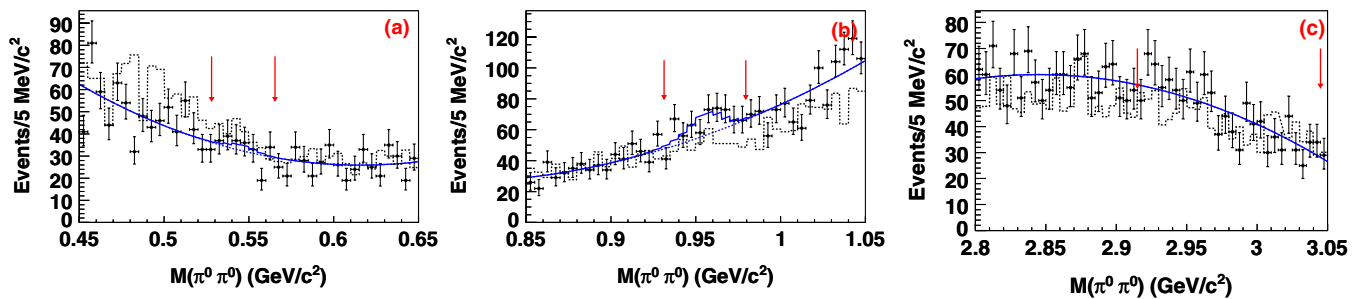


FIG. 2 (color online). (a)–(c): The $\pi^0\pi^0$ invariant mass distributions of the final candidate events in the η , η' , and η_c mass regions, respectively. The dots with error bars are data, the solid lines are the fit described in the text, and the dashed histograms are the sum of all the simulated normalized backgrounds. The arrows show mass regions which contain around 95% of the signal according to MC simulations.

Figure 2 shows the $\pi^0\pi^0$ invariant mass distributions of the final candidate events in the η , η' , and η_c mass regions with the blinded boxes removed, where dots with error bars are data, and the dashed histograms are all the simulated normalized backgrounds. No evident signal is observed, and the simulated backgrounds describe the data well. Since there are no peaking backgrounds in $\eta/\eta'/\eta_c \rightarrow \pi^0\pi^0$, the invariant mass distributions are fit with η , η' , and acceptance-corrected η_c signal shapes obtained from MC simulations and 2nd-order Chebychev functions as background shapes, and 11 ± 18 , 75 ± 30 , and 0.1 ± 14 η , η' , and η_c signal events, respectively, are obtained with the corresponding statistical significances of 0.6σ , 2.6σ , and 0.1σ . The fitted results are shown in Fig. 2 as solid lines.

In the $\eta' \rightarrow \pi^0\pi^0$ invariant mass distribution, a few events accumulate in the signal region. They may from $f_0(980)$ decays, since the process $J/\psi \rightarrow \gamma f_0(980) \rightarrow \gamma\pi^0\pi^0$ is not forbidden, and the $f_0(980)$ mass is not very far from the small peak. But since the signal significance is only 2.6σ and, in the partial wave analysis of $J/\psi \rightarrow \gamma\pi^0\pi^0$, no $f_0(980)$ signal is evident or needed [18], the peak may be due to a statistical fluctuation. To give a conservative measurement on the upper limit and since this was a blind analysis with the background estimated beforehand, the process $J/\psi \rightarrow \gamma f_0(980) \rightarrow \gamma\pi^0\pi^0$ is not considered in the fit.

V. SYSTEMATIC UNCERTAINTIES

The sources of the systematic errors for the branching fraction measurements are summarized in Table I. The uncertainty is negligible for pion identification, since the identification of only one of the pions is required. The uncertainty in the tracking efficiency is 2% per track [19] and is additive. The uncertainty associated with the kinematic fit is determined to be 2% for $\eta/\eta'/\eta_c \rightarrow \pi^+\pi^-$ using the control sample $J/\psi \rightarrow \pi^+\pi^-\pi^0$, while the uncertainty can be neglected for $\eta/\eta'/\eta_c \rightarrow \pi^0\pi^0$, since we require only a very loose χ^2 requirement (the default value is 200). The uncertainty due to photon detection is

TABLE I. Relative systematic errors (%) of the decay branching fractions.

Source	$\eta/\eta'/\eta_c \rightarrow \pi^+\pi^-$	$\eta/\eta'/\eta_c \rightarrow \pi^0\pi^0$
Tracking	4.0	...
Kinematic fit	2.0	...
Photon efficiency	1.0	5.0
π^0 selection	...	2.0
MC statistics	1.4	1.4
EMC energy	0.2	...
and $ \chi_{dE/dx} $ cuts		
Trigger efficiency	...	0.1
Background shape	4.2/6.3/6.6	5.6/5.5/8.8
Branching fractions	3.1/2.9/24	3.1/2.9/24
Resonance parameter	-/-/8.0	-/-/9.5
Number of J/ψ events	1.3	1.3
Sum in quadrature	7.3/8.6/27	8.6/8.5/28

1% per photon. This is determined from studies of photon detection efficiencies in well-understood decays such as $J/\psi \rightarrow \rho^0\pi^0$ and a study of photon conversion via $e^+e^- \rightarrow \gamma\gamma$. The uncertainty due to π^0 selection is determined from a high purity control sample of $J/\psi \rightarrow \pi^+\pi^-\pi^0$ decays. The π^0 selection efficiency is obtained from the change in the π^0 yield in the $\pi^+\pi^-$ recoiling mass spectrum with or without the π^0 selection requirement. The difference of π^0 reconstruction efficiency between data and MC simulation gives an uncertainty of 1% per π^0 [20]. The uncertainties associated with the EMC energy and $|\chi_{dE/dx}|$ requirements are estimated to be 0.2% using the control sample $J/\psi \rightarrow \pi^+\pi^-\pi^0$. According to the MC simulations, the trigger efficiencies for the decays $\eta/\eta'/\eta_c \rightarrow \pi^+\pi^-$ are almost 100%, and the uncertainties are neglected. The systematic uncertainties due to the trigger efficiencies in neutral channels $\eta/\eta'/\eta_c \rightarrow \pi^0\pi^0$ are estimated to be $<0.1\%$, based on cross checks using different trigger conditions. The background uncertainties are evaluated by changing the background fitting function and the fitting range. Errors on the branching fractions of the $J/\psi \rightarrow \gamma\eta/\eta'/\eta_c$ are taken from the PDG [14]. The uncertainty due to the resonance parameters, especially the

η_c width, is estimated by varying the parameters by 1σ . Finally, the uncertainty on the number of J/ψ events is 1.3% [7]. Assuming that all of these systematic error sources are independent, we add them in quadrature to obtain total systematic errors, as shown in Table I.

VI. SUMMARY

Since no evident η , η' , or η_c signal is observed in any decay mode, we determine upper limits on the branching fractions $\mathcal{B}(R \rightarrow \pi\pi)$ ($R = \eta, \eta', \eta_c$) with the following formula

$$\mathcal{B}(R \rightarrow \pi\pi)^{\text{UP}} = \frac{N_{\text{sig}}^{\text{UP}}}{N_{J/\psi} \times \epsilon \times \mathcal{B}(J/\psi \rightarrow \gamma R)},$$

where $N_{\text{sig}}^{\text{UP}}$ is the upper limit on the number of observed events for the signal; ϵ is the detection efficiency obtained from MC simulation, where the radiative M1 photon is distributed according to a $1 + \cos^2\theta$ distribution and multi-hadronic decays of $\eta/\eta'/\eta_c \rightarrow \pi\pi$ are simulated using phase space distributions; and $N_{J/\psi}$ is the total number of J/ψ events, $(225.2 \pm 2.8) \times 10^6$ [7], which is obtained from inclusive hadronic decays. For the decay $R \rightarrow \pi^0\pi^0$, this should be divided by the square of the $\pi^0 \rightarrow \gamma\gamma$ branching fraction, when calculating the branching fraction of $R \rightarrow \pi^0\pi^0$.

Table II lists the final results for the upper limits on the branching fractions of all the processes studied, together with the upper limits on the numbers of signal events, their detection efficiencies, and signal significances. Here, in order to calculate conservative upper limits on these branching fractions, the efficiencies have been lowered by a factor of $1 - \sigma_{\text{sys}}$. For comparison, we also list the best upper limits on $\eta/\eta'/\eta_c$ decays to $\pi^+\pi^-$ and $\pi^0\pi^0$ states to date from the PDG [14]. Except for $\mathcal{B}(\eta \rightarrow \pi\pi)$, where the KLOE and GAMS-4 π Collaborations have huge η samples providing the lowest upper limits for $\eta \rightarrow \pi^+\pi^-$ and $\eta \rightarrow \pi^0\pi^0$, our upper limits are the lowest. These results provide experimental limits for theoretical

TABLE II. Summary of the limits on $\eta/\eta'/\eta_c$ decays to $\pi^+\pi^-$ and $\pi^0\pi^0$ states. $N_{\text{sig}}^{\text{UP}}$ is the upper limit on the number of signal events, ϵ is the efficiency, σ_{sys} is the total systematic error, S is the number of statistical significance, \mathcal{B}^{UP} is the upper limit at the 90% confidence level on the decay branching fraction of $\eta/\eta'/\eta_c$ to $\pi^+\pi^-$ or $\pi^0\pi^0$, and $\mathcal{B}_{\text{PDG}}^{\text{UP}}$ is the upper limit on the decay branching fraction from PDG [14].

Process	$N_{\text{sig}}^{\text{UP}}$	ϵ (%)	σ_{sys} (%)	S	\mathcal{B}^{UP}	$\mathcal{B}_{\text{PDG}}^{\text{UP}}$
$\eta \rightarrow \pi^+\pi^-$	48	54.28	7.3	0.8σ	3.9×10^{-4}	1.3×10^{-5}
$\eta' \rightarrow \pi^+\pi^-$	32	53.81	8.6	0.1σ	5.5×10^{-5}	2.9×10^{-3}
$\eta_c \rightarrow \pi^+\pi^-$	92	25.27	27	1.5σ	1.3×10^{-4}	6×10^{-4}
$\eta \rightarrow \pi^0\pi^0$	36	23.75	8.6	0.6σ	6.9×10^{-4}	3.5×10^{-4}
$\eta' \rightarrow \pi^0\pi^0$	110	23.18	8.5	2.6σ	4.5×10^{-4}	9×10^{-4}
$\eta_c \rightarrow \pi^0\pi^0$	40	35.70	28	0.1σ	4.2×10^{-5}	4×10^{-4}

models, predicting how much CP and P violation there may be in η' and η_c meson decays.

ACKNOWLEDGMENTS

The BESIII Collaboration thanks the staff of BEPCII and the computing center for their hard efforts. This work is supported in part by the Ministry of Science and Technology of China under Contract No. 2009CB825200; National Natural Science Foundation of China (NNSFC) under Contracts No. 10625524, No. 10821063, No. 10825524, No. 10835001, and No. 10935007; the Chinese Academy of Sciences (CAS) Large-Scale

Scientific Facility Program; CAS under Contracts No. KJCX2-YW-N29 and No. KJCX2-YW-N45; 100 Talents Program of CAS; Istituto Nazionale di Fisica Nucleare, Italy; Siberian Branch of the Russian Academy of Science, joint project No. 32 with CAS; U. S. Department of Energy under Contracts No. DE-FG02-04ER41291, No. DE-FG02-91ER40682, and No. DE-FG02-94ER40823; University of Groningen (RuG) and the Helmholtzzentrum fuer Schwerionenforschung GmbH (GSI), Darmstadt; and the WCU Program of the National Research Foundation of Korea under Contract No. R32-2008-000-10155-0.

-
- [1] C. Jarlskog and E. Shabalin, *Phys. Scr.* **T99**, 23 (2002); E. Shabalin, *ibid.* **T99**, 104 (2002).
- [2] F. Ambrosino *et al.* (KLOE Collaboration), *Phys. Lett. B* **606**, 276 (2005).
- [3] T. Mori *et al.* (Belle Collaboration), *J. Phys. Soc. Jpn.* **76**, 074102 (2007).
- [4] M. Ablikim *et al.* (BES Collaboration), *Eur. Phys. J. C* **45**, 337 (2006).
- [5] A. M. Blik *et al.*, *Phys. At. Nucl.* **70**, 693 (2007).
- [6] D. Alde *et al.* (LAPP Collaboration), *Z. Phys. C* **36**, 603 (1987).
- [7] M. Ablikim *et al.* (BESIII Collaboration), *Phys. Rev. D* **83**, 012003 (2011).
- [8] M. Ablikim *et al.* (BES Collaboration), *Nucl. Instrum. Methods Phys. Res., Sect. A* **614**, 345 (2010).
- [9] J. Z. Bai *et al.* (BES Collaboration), *Nucl. Instrum. Methods Phys. Res., Sect. A* **344**, 319 (1994); **458**, 627 (2001).
- [10] D. M. Asner *et al.*, *Int. J. Mod. Phys. A* **24**, 499 (2009).
- [11] Z. Y. Deng *et al.*, *Chinese Phys. C* **30**, 371 (2006).
- [12] S. Jadach, B. F. L. Ward, and Z. Was, *Comput. Phys. Commun.* **130**, 260 (2000); *Phys. Rev. D* **63**, 113009 (2001).
- [13] R. G. Ping *et al.*, *Chinese Phys. C* **32**, 599 (2008).
- [14] K. Nakamura *et al.* (Particle Data Group), *J. Phys. G* **37**, 075021 (2010).
- [15] J. C. Chen, G. S. Huang, X. R. Qi, D. H. Zhang, and Y. S. Zhu, *Phys. Rev. D* **62**, 034003 (2000).
- [16] W. D. Li *et al.*, in *Proceedings of CHEP06, Mumbai, India, 2006* (unpublished).
- [17] Ying-Jia Gao, Yu-Jie Zhang, and Kuang-Ta Chao, [arXiv: hep-ph/0701009](https://arxiv.org/abs/hep-ph/0701009).
- [18] M. Ablikim *et al.* (BES Collaboration), *Phys. Lett. B* **642**, 441 (2006).
- [19] M. Ablikim *et al.* (BESIII Collaboration), *Phys. Rev. D* **83**, 112005 (2011).
- [20] M. Ablikim *et al.* (BES Collaboration), *Phys. Rev. D* **81**, 052005 (2010).